Takagi–Sugeno Fuzzy Unknown Input Observers to Estimate Nonlinear Dynamics of Autonomous Ground Vehicles: Theory and Real-Time Verification

Tran Anh-Tu Nguyen, Truong Quang Dinh, Thierry-Marie Guerra, Juntao Pan

Takagi–Sugeno Fuzzy Unknown Input Observers to Estimate Nonlinear Dynamics of Autonomous Ground Vehicles: Theory and Real-Time Verification

Article *in* IEEE/ASME Transactions on Mechatronics · June 2021

DOI: 10.1109/TMECH.2020.3049070

CITATIONS
29

READS
728

4 authors, including:

Anh-Tu Nguyen
Université Polytechnique Hauts-de-France
140 PUBLICATIONS **2,084** CITATIONS

SEE PROFILE

Thierry-Marie Guerra
Université Polytechnique Hauts-de-France
349 PUBLICATIONS **9,873** CITATIONS

SEE PROFILE

Takagi-Sugeno Fuzzy Unknown Input Observers to Estimate Nonlinear Dynamics of Autonomous Ground Vehicles: Theory and Real-Time Verification

Anh-Tu Nguyen*, *Member, IEEE*, Truong Quang Dinh, *Senior Member, IEEE*, Thierry-Marie Guerra, Juntao Pan

***Abstract*—We address the *simultaneous* estimation problem of the lateral speed, the steering input and the effective engine torque, which play a fundamental role in vehicle handling, stability control and fault diagnosis of autonomous ground vehicles. Due to the involved longitudinal-lateral coupling dynamics and the presence of unknown inputs (UIs), a new nonlinear observer design technique is proposed to guarantee the asymptotic estimation performance. To this end, we make use of a specific Takagi-Sugeno (TS) fuzzy representation with nonlinear consequents to *exactly* model the nonlinear vehicle dynamics within a compact set of the vehicle state. This TS fuzzy modeling not only allows reducing significantly the real-time computational effort in estimating the vehicle variables but also enables an effective way to deal with unmeasured nonlinearities. Moreover, via a *generalized* Luenberger observer structure, the UI decoupling can be achieved without requiring *a priori* UI information. Using Lyapunov stability arguments, the UI observer design is reformulated as an optimization problem under linear matrix inequalities, which can be effectively solved with standard numerical solvers. The effectiveness of the proposed TS fuzzy UI observer design is demonstrated with real-time hardware-in-the-loop experiments.**

***Index Terms*—Vehicle dynamics, nonlinear observers, vehicle state estimation, steering angle estimation, torque estimation, Takagi-Sugeno fuzzy systems.**

I. Introduction

REAL-time knowledge on the vehicle dynamics and the driver-related variables is essential for active safety control [1], vehicle fault detection and diagnosis [2], and driver-vehicle monitoring systems [3] of autonomous ground vehicles. Unfortunately, the onboard vehicle sensors are not always available onboard due to economical and/or technical reasons [4], [5]. In particular, within some specific situations, the human driver variables cannot be directly measured by physical sensors [6]. Hence, developing estimation algorithms to reconstruct the vehicle dynamics from the online information of low-cost sensors has received an ever-increasing interest worldwide [6]–[8].

The information on the lateral speed or the sideslip angle is a crucial index for vehicle handling and lateral stability. However, commercial physical sensors to measure the lateral speed are expensive, which cannot be directly used in practice [9]. Hence, a great deal of research efforts has been devolved to the lateral speed estimation [4], [9]–[11]. An industrially amenable kinematic-based approach has been proposed in [12]. Without requiring tire–road friction parameters or other dynamical vehicle properties, this method can lead to the drift phenomena induced by bias errors [4]. Kalman filtering methods have been widely exploited for estimating sideslip angle, especially within nonlinear estimation context [13]–[16]. Despite their effectiveness, these methods require a fine tuning task and *a priori* information on the noises affected to the vehicles to achieve a satisfactory estimation performance. To overcome these drawbacks, robust observers based on dynamical vehicle properties have been proposed [4], [17], [18]. However, the design of robust observers becomes challenging in presence of nonlinear dynamics and/or unknown disturbances, which is unavoidable for critical driving situations [12]. By exploiting the key features of different low-cost sensors, fusion-data-based techniques have been proved as an effective technique to estimate the vehicle sideslip angle [19]–[21]. However, such techniques induce additional sensor costs and complexities for estimation algorithms [12]. It is important to emphasize that the longitudinal-lateral coupling has been ignored in most of model-based estimation methods [13]. The main reason is due to the challenges involved in the corresponding nonlinear observer design [10].

Since the steering angle directly controls the vehicle direction, this variable is a fundamental input for path tracking control, path planning, active safety control and also detection of driver failure of intelligent vehicles [1], [22]. The steering angle can be precisely measured with absolute rotary encoders, which are quite expensive and fragile to most of passenger vehicles [10]. The low-cost sensors may lead to faulty measurement results or provide erroneous steering signals. Hence, the estimation of the steering angle has attracted increasing research attention. Based on the information from the global positioning system (GPS) and the micro-electromechanical

This work was supported in part by the French Ministry of Higher Education and Research; in part by the National Center for Scientific Research (CNRS); in part by the Nord-Pas-de-Calais Region under Project ELSAT 2020; in part by Key Research Project of North Minzu University under Grant 2019KJ39; in part by the Natural Science Foundation of Ningxia Hui Autonomous Region under Grant 2019AAC03118; in part by the National Natural Science Foundation of China under Grant 61463001; in part by the Major Special Project of North Minzu University under Grant ZDZX201902; in part by the Third Batch of Ningxia Youth Talents Supporting Program under Grant TJGC2018097; in part by the Advanced Intelligent Perception and Control Technology Innovative Team of Ningxia.

A.-T. Nguyen and T.-M. Guerra are with the LAMIH laboratory, UMR CNRS 8201, Université Polytechnique Hauts-de-France, Valenciennes, France (e-mail: nguyen.trananhtu@gmail.com; thierry.guerra@uphf.fr). A.-T. Nguyen is also with the INSA Hauts-de-France, Valenciennes, France.

T. Dinh is with the University of Warwick, Coventry, UK (e-mail: t.dinh@warwick.ac.uk).

J. Pan is with the School of Electrical and Information Engineering, North Minzu University, Yinchuan, China (e-mail: jtpan@aliyun.com).

*Corresponding author: Anh-Tu Nguyen.

system (MEMS), an unscented Kalman filter has been proposed in [23] to estimate the steering angle for agricultural tractors. A linear extended observer has been proposed in [24] for steering angle estimation, which is then exploited to reconstruct the road curvature signal for vehicle lateral control. The effective engine torque is also crucial for various automotive applications, *e.g.*, brake torque control, speed control, adaptive cruise control [25]. However, it is difficult to directly measure this vehicle variable for commercial cars due to both economic and technical reasons [26]. Then, the effective engine torque is generally supplied in the form of look-up-tables (LUTs) as a function of in-cylinder air flow rate, engine speed, injected fuel, etc., which are established and calibrated by steady-state engine tests [26], [27]. To reduce the costs for development, testing, maintenance, and robustness related to LUTs-based estimations, various model-based algorithms have been developed to estimate the effective engine torque. High-order sliding mode observer has been proposed in [28] to estimate the engine friction torque and load torque. Based on the principles of Kalman filtering, a method has been developed in [29] for estimating the engine combustion torque. A two-step observer design, requiring different intake air measurement sensors and real-time engine speed, has been proposed to estimate the real-time engine torque [30]. Na *et al.* [31] have proposed an unknown input observer for online estimation of unknown effective engine torque with measured engine speed, load torque and air mass flow rate.

Despite significant advances on vehicle estimation techniques, *simultaneous* estimation of both the sideslip angle and the steering angle as well as the effective engine torque has not been achieved. The significance of such an estimation solution is multi-fold. First, the estimated sideslip angle can be used for vehicle active safety control [1], while the estimates of the steering angle and the effective engine torque are useful for fault diagnosis of intelligent automotive systems [2]. Second, the proposed estimation solution is cost-effective since it only requires the online information from low-cost sensors. These issues motivate the new observer design method in this paper. The proposed unknown input (UI) observer design is based on a combined longitudinal-lateral vehicle model, whose steering angle and effective engine torque are considered as UIs. Two design challenges arise concerning: (1) dealing with the *unmeasured* nonlinearities of vehicle dynamics, (2) guaranteeing an asymptotic convergence of both the vehicle state and the UIs. To meet similar challenges, Takagi-Sugeno (TS) fuzzy model-based techniques [32], [33] have been attempted to design nonlinear UI observers [10], [34]. However, based on the Lipschitz property of the membership functions (MFs), the existing results generally lead to over-conservative results or complex observer design frameworks [35]. Note also that due to technical challenges related to dealing with unmeasured MFs, fuzzy UI observer design and fuzzy fault detection/diagnosis have been mainly focused on systems with measurable nonlinearities [34], which is not the case of the considered nonlinear vehicle dynamics. The following contributions of this paper can overcome the above-mentioned drawbacks.

- The nonlinear vehicle system is equivalently rewritten in a *specific* TS fuzzy form with both measured and unmeasured nonlinear consequents. Hence, the number of TS local subsystems, directly related to the real-time computational cost, can be significantly reduced [36]. Moreover, this TS fuzzy form permits an effective application of the differential mean value theorem [37] to deal with unmeasured nonlinearities.
- Using a *generalized* Luenberger observer structure, an effective UI decoupling can be achieved. Hence, an asymptotic estimation convergence of both the vehicle state and UIs can be guaranteed via Lyapunov stability without requiring any *a priori* UI information [34] or any specific choice of UI matrix [10]. The UI observer design is recast as a convex optimization problem under linear matrix inequality (LMI) constraints, effectively solved with standard numerical solvers.
- The effectiveness of the proposed fuzzy UI observer framework is practically verified with real-time hardware-in-the-loop (HiL) experiments.

Notation. The set of nonnegative integers is denoted by $\mathbb{Z}_+$ and $\mathcal{I}_r = \{1, 2, \ldots, r\} \subset \mathbb{Z}_+$. For $i \in \mathcal{I}_r$, we denote $\xi_r(i) = [0, \ldots, 0, \overbrace{1}^{i\text{th}}, 0, \ldots, 0]^\top \in \mathbb{R}^r$ a vector of the canonical basis of $\mathbb{R}^r$. For a vector x, x_i denotes its ith entry. For two vectors $x, y \in \mathbb{R}^n$, the convex hull of these vectors is denoted as $\mathrm{co}(x, y) = \{\lambda x + (1-\lambda)y : \ \lambda \in [0, 1]\}$. For a matrix X, $X^\top$ denotes its transpose, $X \succ 0$ means X is positive definite, and $\mathrm{He}X = X + X^\top$. When the existence is guaranteed, $X^\dagger$ denotes the Moore–Penrose pseudo-inverse of matrix X, *i.e.*, $X^\dagger = \left(X^\top X\right)^{-1} X^\top$. $\mathrm{diag}(X_1, X_2)$ denotes a block-diagonal matrix composed of X_1, X_2. I denotes the identity matrix of appropriate dimension. In block matrices, the symbol $\star$ stands for the terms deduced by symmetry. Arguments are omitted when their meaning is clear.

II. Vehicle Modeling and Problem Formulation

This section presents the nonlinear vehicle model used for UI observer design. Then, the related observer problem is formulated. The vehicle nomenclature is given in Table I.

TABLE I
Parameter Values of Vehicle Model.

Parameter	Description	Value
M	Vehicle mass	1476 [kg]
l_f	Distance from gravity center to front axle	1.13 [m]
l_r	Distance from gravity center to rear axle	1.49 [m]
I_e	Effective longitudinal inertia	442.8 [kgm^2]
I_z	Vehicle yaw moment of inertia	1810 [kgm^2]
C_f	Front cornering stiffness	57000 [N/rad]
C_r	Rear cornering stiffness	59000 [N/rad]
C_x	Longitudinal aerodynamic drag coefficient	0.35 [–]
C_y	Lateral aerodynamic drag coefficient	0.45 [–]

A. Nonlinear Vehicle Model

Fig. 1 depicts a two degrees-of-freedom vehicle model. This model represents the vehicle motion in the horizontal plane,

whose dynamics is described as follows [38]:

$$\begin{aligned}\dot{v}_x &= \frac{T_{eng} - C_x v_x^2}{I_e} + v_y r \\ \dot{v}_y &= \frac{F_{yf} + F_{yr} - C_y v_y^2}{M} - v_x r \\ \dot{r} &= \frac{l_f F_{yf} - l_r F_{yr}}{I_z}\end{aligned} \tag{1}$$

where v_x is the vehicle longitudinal speed, v_y is the lateral speed, r is the vehicle yaw rate, and T_{eng} represents the torque input for the vehicle longitudinal dynamics [1]. The cornering forces at the front tires F_{yf} and at the rear tires F_{yr} are modeled using the magic formula [7] as

$$\begin{aligned}F_{yi}(\alpha_i) &= \mathcal{D}_i \sin(\nabla_i), \quad i \in \{f, r\} \\ \nabla_i &= \mathcal{C}_i \arctan[(1-\mathcal{E}_i)\mathcal{B}_i\alpha_i + \mathcal{E}_i \arctan(\mathcal{B}_i\alpha_i))],\end{aligned} \tag{2}$$

where the Pacejka parameters $\mathcal{B}_i$, $\mathcal{C}_i$, $\mathcal{D}_i$ and $\mathcal{E}_i$ depend on the characteristics of the tire, the road and the vehicle operating conditions. Note that the Pacejka tire model (2) is used for simulation validation purposes in Section IV. The wheel slip angles for the front and rear tires are modeled as follows [1]:

$$\alpha_f = \delta - \arctan\left(\frac{v_y + l_f r}{v_x}\right), \quad \alpha_r = \arctan\left(\frac{l_r r - v_y}{v_x}\right),$$

where δ is the front wheel steering angle.

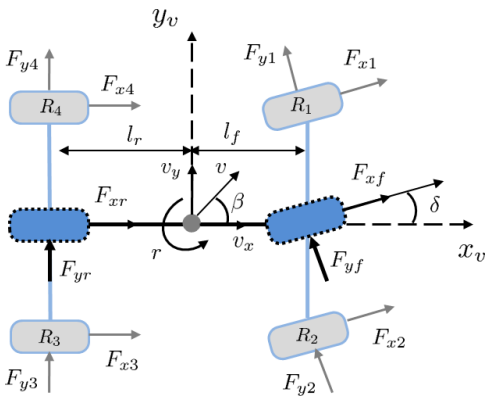

Fig. 1. Schematic of a two degrees-of-freedom vehicle model.

B. Observer Problem Statement

For observer design, we consider the normal driving situation with small angle assumption [1], [3], [9]. Moreover, the lateral tire forces are proportional to the slip angles of each axle. Hence, the lateral tire forces (2) can be approximated by

$$F_{yf} = 2C_f\left(\delta - \frac{v_y + l_f r}{v_x}\right), \; F_{yr} = 2C_r\left(\frac{l_r r - v_y}{v_x}\right), \tag{3}$$

From (1) and (3), the nonlinear vehicle dynamics used for observer design can be obtained as follows:

$$\dot{x} = A_v(x)x + D_v d, \tag{4}$$

where $x = \begin{bmatrix} v_x & v_y & r \end{bmatrix}^\top$ is the vehicle state vector, $d = \begin{bmatrix} T_{eng} & \delta \end{bmatrix}^\top$ is the control input. The state-space matrices of the nonlinear vehicle model (4) are given by

$$A_v(x) = \begin{bmatrix} a_{11} & 0 & v_y \\ 0 & a_{22} & a_{23} \\ 0 & a_{32} & a_{33} \end{bmatrix}, \quad D_v = \begin{bmatrix} d_{11} & 0 \\ 0 & d_{22} \\ 0 & d_{32} \end{bmatrix},$$

with

$$\begin{aligned} a_{11} &= -\frac{C_x v_x}{I_e}, & d_{11} &= \frac{1}{I_e} \\ a_{22} &= -\frac{2(C_f + C_r)}{M v_x} - \frac{C_y v_y}{M}, & a_{23} &= \frac{2(C_r l_r - C_f l_f)}{M v_x} - v_x \\ a_{32} &= \frac{2(l_r C_r - C_f l_f)}{I_z v_x}, & a_{33} &= -\frac{2(C_f l_f^2 + C_r l_r^2)}{I_z v_x} \\ d_{22} &= \frac{2C_f}{M}, & d_{32} &= \frac{2 l_f C_f}{I_z}. \end{aligned}$$

Taking into account the physical limitations during normal driving conditions [3], the compact set of the vehicle state is defined as

$$\mathscr{D}_x = \left\{ v_x \in [\underline{v}_x, \overline{v}_x], \; v_y \in [\underline{v}_y, \overline{v}_y], \; r \in [\underline{r}, \overline{r}] \right\}. \tag{5}$$

where $\underline{v}_x = 5$ [m/s], $\overline{v}_x = 30$ [m/s], $\underline{v}_y = -1.5$ [m/s], $\overline{v}_y = 1.5$ [m/s], $\underline{r} = -0.55$ [rad/s] and $\overline{r} = 0.55$ [rad/s]. For system (4), we assume that the vehicle speed v_x [m/s] and the yaw rate r [rad/s] can be directly measured whereas the measurement of the lateral speed v_y [m/s] is not available. Hence, the output equation of system (4) is given by

$$y = Cx, \quad C = \begin{bmatrix} 1 & 0 & 0 \\ 0 & 0 & 1 \end{bmatrix}. \tag{6}$$

In this work, the steering angle δ and the effective engine torque T_{eng} are considered as unknown inputs to be estimated.

The vehicle system (4) has three nonlinearities (or premise variables), *i.e.*, v_x, $\frac{1}{v_x}$ and v_y. Using the sector nonlinearity approach [32, Chapter 2], a classical eight-rule TS fuzzy model of the nonlinear vehicle dynamics (4) can be easily derived as

$$\dot{x} = \sum_{i=1}^{8} h_i(z) A_i x + D_v d, \quad y = Cx, \tag{7}$$

where $z = \begin{bmatrix} v_x & \frac{1}{v_x} & v_y \end{bmatrix}^\top$ is the vector of premise variables. The local state-space matrices A_i, and the corresponding MFs $h_i(z)$ of the TS fuzzy model (7), for $i \in \mathcal{I}_8$, are not given here for brevity. Similar TS fuzzy representations as (7) have been used for vehicle dynamics estimation, see for instance [10]. However, this classical TS fuzzy form (7) leads to both theoretical and practical difficulties [35].

- Due to the practical unavailability of v_y, the MFs $h_i(z)$, for $i \in \mathcal{I}_8$, are unmeasured. Designing TS fuzzy observers in this situation still remains challenging [35], especially in presence of unknown inputs [10].
- The classical TS model (7) may yield a TS fuzzy observer with complex structure for real-time implementation.

To overcome these drawbacks, we reformulate the vehicle system (4) in the following form:

$$\begin{aligned}\dot{x} &= A(\xi)x + D_v d + f_v(\xi) + G_v\phi(x), \\ y &= Cx,\end{aligned} \tag{8}$$

where $\phi(x) = v_y^2$, and

$$A(\xi) = \begin{bmatrix} 0 & r & 0 \\ 0 & -\frac{2(C_f+C_r)}{Mv_x} & 0 \\ 0 & \frac{2(l_rC_r-C_fl_f)}{I_zv_x} & 0 \end{bmatrix}, \qquad \xi = \begin{bmatrix} \frac{1}{v_x} \\ r \end{bmatrix},$$

$$f_v(\xi) = \begin{bmatrix} -\frac{C_xv_x^2}{I_e} \\ \frac{2(C_rl_r-C_fl_f)r}{Mv_x} - v_xr \\ -\frac{2(C_fl_f^2+C_rl_r^2)r}{I_zv_x} \end{bmatrix}, \qquad G_v = \begin{bmatrix} 0 \\ -\frac{C_y}{M} \\ 0 \end{bmatrix}.$$

In this paper, we perform the observer design in the discrete-time domain for real-time implementation. To this end, Euler's discretization method, with the sampling time $T_s = 0.01$ [s], is used to obtain the discrete-time model of system (8) as

$$\begin{aligned} x_{k+1} &= A(\xi_k)x_k + Dd_k + f(\xi_k) + G\phi(x_k), \\ y_k &= Cx_k, \end{aligned} \tag{9}$$

where

$$\begin{aligned} A(\xi_k) &= T_sA_v(\xi_k) + I, \quad G = T_sG_v, \\ f(\xi_k) &= T_sf_v(\xi_k), \qquad\quad D = T_sD_v. \end{aligned}$$

For convenience of presentation, we explicitly denote $A(\xi) = A(V_x, r)$ with $V_x = \frac{1}{v_x} \in [\underline{V}_x, \overline{V}_x]$. Using the sector nonlinearity approach [32] with the premise vector $\xi \in \mathbb{R}^2$, the following four-rule TS model of system (9) can be derived:

$$\begin{aligned} x_{k+1} &= \sum_{i=1}^{4} h_i(\xi_k)A_ix_k + Dd_k + f(\xi_k) + G\phi(x_k), \\ y_k &= Cx_k, \end{aligned} \tag{10}$$

where the local matrices A_i, for $i \in \mathcal{I}_4$, are given by

$$\begin{aligned} A_1 &= A\left(\underline{V}_x, \underline{r}\right), \quad A_2 = A\left(\underline{V}_x, \overline{r}\right), \\ A_3 &= A\left(\overline{V}_x, \underline{r}\right), \quad A_4 = A\left(\overline{V}_x, \overline{r}\right). \end{aligned}$$

The corresponding membership functions $h_i(\xi_k)$, for $i \in \mathcal{I}_4$, of the TS fuzzy model (10) are defined as

$$\begin{aligned} h_1(\xi) &= \Omega_{v1}\Omega_{r1}, \quad h_2(\xi) = \Omega_{v1}\Omega_{r2}, \\ h_3(\xi) &= \Omega_{v2}\Omega_{r1}, \quad h_4(\xi) = \Omega_{v1}\Omega_{r1}, \end{aligned} \tag{11}$$

with

$$\begin{aligned} \Omega_{v1} &= \frac{\overline{V}_x - V_x}{\overline{V}_x - \underline{V}_x}, \quad \Omega_{r1} = \frac{\overline{r} - r}{\overline{r} - \underline{r}}, \\ \Omega_{v2} &= \frac{V_x - \underline{V}_x}{\overline{V}_x - \underline{V}_x}, \quad \Omega_{r2} = \frac{r - \underline{r}}{\overline{r} - \underline{r}}. \end{aligned}$$

Remark 1. The reformulated vehicle model (8) has two features deserving particular attention. First, the unmeasurable nonlinearity is *isolated* in $\phi(x_k)$. Then, the membership functions $h_i(\xi_k)$, for $i \in \mathcal{I}_4$, defined in (11), of the TS fuzzy model (10) only depend on the measured premise vector ξ_k. Hence, these membership functions can be directly used to construct the UI observer structure as in (16). Note that using the classical TS fuzzy modeling, the membership functions $h_i(z)$, for $i \in \mathcal{I}_8$, of the TS fuzzy model (7) cannot be directly incorporated into the UI observer structure due to their dependency on the unmeasured lateral speed v_y. This induces major technical challenges in designing effective UI observers for systems with unmeasured nonlinearities [10]. Second, a part of nonlinearities are retained in the measured consequent $f(\xi_k)$ and unmeasured consequent $\phi(x_k)$. Hence, the resulting TS observer can be of much simpler structure, *i.e.*, with only four fuzzy rules in place of eight-rule conservative TS representation (7). As shown in the next section, these features enable an effective framework for TS fuzzy UI observer design in terms of dealing with unmeasured nonlinearities and complexity reduction.

This paper provides an effective algorithm for the following vehicle dynamics estimation problem.

Problem 1. Consider the vehicle nonlinear model (10) with the compact set $\mathscr{D}_x$ defined in (5). Design an UI observer such that the lateral speed v_y, the steering action δ and the engine torque T_{eng} can be *asymptotically* and *simultaneously* estimated from the output information (6).

III. UI Observer Design for TS Fuzzy Systems with Unmeasured Nonlinear Consequents

This section presents a new framework to design UI observers for a generalized class of TS fuzzy systems.

A. Observer Structure and Useful Lemmas

For generality, we consider the TS fuzzy system (10) in a more general form

$$\begin{aligned} x_{k+1} &= A(h)x_k + Dd_k + f(\xi_k, u_k) + G(h)\phi(x_k, u_k), \\ y_k &= Cx_k, \end{aligned} \tag{12}$$

where $x_k \in \mathscr{D}_x \subseteq \mathbb{R}^{n_x}$ is the state vector, $u_k \in \mathscr{D}_u \subseteq \mathbb{R}^{n_u}$ is the *known* input, $d_k \in \mathbb{R}^{n_d}$ is the *unknown* input, $y_k \in \mathbb{R}^{n_y}$ is the output vector, and $\xi_k \in \mathbb{R}^{n_\xi}$ is the vector *measured* premise variables. The nonlinear functions $f : \mathscr{D}_x \times \mathscr{D}_u \to \mathbb{R}^{n_x}$ and $\phi : \mathscr{D}_x \times \mathscr{D}_u \to \mathbb{R}^{n_\phi}$ are differentiable with respect to the state x_k. The elements of function $f(\cdot)$ are measurable whereas those of $\phi(\cdot)$ cannot be measured from the output. The state-space matrices of system (12) are given by

$$\begin{bmatrix} A(h) & G(h) \end{bmatrix} = \sum_{i=1}^{N} h_i(\xi_k) \begin{bmatrix} A_i & G_i \end{bmatrix}.$$

Note that the MFs satisfy the following convex sum property:

$$\sum_{i=1}^{N} h_i(\xi_k) = 1, \quad 0 \le h_i(\xi_k) \le 1, \quad \forall i \in \mathcal{I}_N. \tag{13}$$

Let $\mathscr{H}$ be the set of membership functions satisfying (13), *i.e.*, $h = \left[h_1(\xi_k), h_2(\xi_k), \ldots, h_r(\xi_k)\right]^\top \in \mathscr{H}$. The following assumptions are considered for the TS fuzzy system (12).

Assumption 1. The differentiable function $\phi(x_k, u_k)$ satisfies the following boundedness condition:

$$\underline{\rho}_{ij} \le \frac{\partial \phi_i}{\partial x_j}(x, u) \le \overline{\rho}_{ij}, \tag{14}$$

with $\underline{\rho}_{ij} = \min\limits_{\rho \in \mathscr{D}_x \times \mathscr{D}_u} \left(\frac{\partial \phi_i}{\partial x_j}(\rho)\right)$, $\overline{\rho}_{ij} = \max\limits_{\rho \in \mathscr{D}_x \times \mathscr{D}_u} \left(\frac{\partial \phi_i}{\partial x_j}(\rho)\right)$, for $\forall (i,j) \in \mathcal{I}_{n_\phi} \times \mathcal{I}_{n_x}$.

Note that the state x_k and the input u_k of engineering systems are always physically bounded, *i.e.*, $x_k \in \mathscr{D}_x$ and $u_k \in \mathscr{D}_u$. Then, the bounds $\underline{\rho}_{ij}$ and $\overline{\rho}_{ij}$ in (14) can be easily computed.

Assumption 2. We assume that

$$\operatorname{rank}(CD) = \operatorname{rank}(D), \tag{15a}$$

$$\operatorname{rank}\begin{bmatrix} I & D \\ C & 0 \end{bmatrix} = n_x + n_d. \tag{15b}$$

The rank conditions in (15) are standard in UIO design framework for unknown input decoupling [10], [34], [39], [40]. Note that the vehicle nonlinear system (10) verifies these rank conditions.

For estimation purposes, we consider the following UI observer structure:

$$\zeta_{k+1} = \mathscr{T}\hat{\Phi}_k + \mathscr{L}(h)(y_k - \hat{y}_k), \tag{16a}$$

$$\hat{x}_k = \zeta_k + \mathscr{N} y_k, \tag{16b}$$

$$\hat{d}_k = (CD)^{\dagger}(y_{k+1} - C\hat{\Phi}_k), \tag{16c}$$

with $\hat{\Phi}_k = A(h)\hat{x}_k + f(\xi_k, u_k) + G(h)\phi(\hat{x}_k, u_k)$. The existence of the Moore–Penrose pseudo-inverse matrix $(CD)^{\dagger}$ is guaranteed by condition (15a). The matrices $\mathscr{T} \in \mathbb{R}^{n_x \times n_x}$, $\mathscr{N} \in \mathbb{R}^{n_x \times n_y}$ and $\mathscr{L}(h) \in \mathbb{R}^{n_x \times n_y}$ are to be designed with

$$\mathscr{T} + \mathscr{N}C = I. \tag{17}$$

Remark 2. Note that selecting $\mathscr{T} = I$ and $\mathscr{N} = 0$, the UI observer structure (16) reduces to the well-known Luenberger observer [41], widely used in the literature.

From the matrix constraint (17), it follows that

$$x_{k+1} = \mathscr{T}x_{k+1} + \mathscr{N}Cx_{k+1} = \mathscr{T}x_{k+1} + \mathscr{N}y_{k+1}. \tag{18}$$

Then, from (12) and (18), the dynamics of the TS fuzzy system can be rewritten as

$$\begin{aligned} x_{k+1} = {} & \mathscr{T}A(h)x_k + \mathscr{T}Dd_k + \mathscr{T}f(\xi_k, u_k) \\ & + \mathscr{T}G(h)\phi(x_k, u_k) + \mathscr{N}y_{k+1}. \end{aligned} \tag{19}$$

Let us define the state estimation error as $e_k = x_k - \hat{x}_k$. To achieve an asymptotic state estimation, we impose

$$\mathscr{T}D = 0. \tag{20}$$

Then, the estimation error dynamics can be defined from (16a), (16b), (19) and (20) as

$$\begin{aligned} e_{k+1} &= x_{k+1} - \hat{x}_{k+1} \\ &= x_{k+1} - \zeta_{k+1} - \mathscr{N}y_{k+1} \\ &= \mathscr{T}A(h)e_k + \mathscr{T}G(h)\delta_\phi - \mathscr{L}(h)Ce_k, \end{aligned} \tag{21}$$

where $\delta_\phi = \phi(x_k, u_k) - \phi(\hat{x}_k, u_k)$. The mismatching nonlinear term δ_ϕ caused by the unmeasured premise variables leads to technical difficulties in designing TS fuzzy observers [35]. To effectively deal with this term and achieve an asymptotic error convergence, the following lemma is useful to rewrite δ_ϕ as a function of e_k.

Lemma 1 (Differential Mean Value Theorem [37])**.** Let $g(x) : \mathbb{R}^{n_x} \to \mathbb{R}^q$ and $a, b \in \mathbb{R}^{n_x}$. If $g(x)$ is differentiable on $\operatorname{co}(a, b)$, then there exist constant vectors $c_i \in \operatorname{co}(a, b)$, $c_i \neq a$, $c_i \neq b$, for $\forall i \in \mathcal{I}_q$, such that

$$g(a) - g(b) = \left(\sum_{i=1}^{q} \sum_{j=1}^{n_x} \sigma_q(i)\sigma_{n_x}^{\top}(j) \frac{\partial g_i}{\partial x_j}(c_i) \right)(a - b).$$

Applying Lemma 1 to function $\phi(x_k, u_k)$, then there exist $\vartheta_i \in \operatorname{co}(x_k, \hat{x}_k)$, for $i \in \mathcal{I}_{n_\phi}$, such that

$$\delta_\phi = \left(\sum_{i=1}^{n_\phi} \sum_{j=1}^{n_x} \sigma_{n_\phi}(i)\sigma_{n_x}^{\top}(j) \frac{\partial \phi_i}{\partial x_j}(\vartheta_i, u) \right)(x - \hat{x}). \tag{22}$$

We denote $\theta_{ij} = \frac{\partial \phi_i}{\partial x_j}(\vartheta_i, u)$, for $\forall (i, j) \in \mathcal{I}_{n_\phi} \times \mathcal{I}_{n_x}$, and

$$\theta = \left[\theta_{11}, \ldots, \theta_{1n_x}, \ldots, \theta_{n_\phi n_x}\right].$$

Due to the boundedness condition (14), the unknown parameter θ belongs to a bounded convex set $\mathscr{S}_\phi$, whose set of $2^{n_\phi n_x}$ vertices is given by

$$\mathscr{V}_\phi = \{\theta = \left[\theta_{11}, \ldots, \theta_{1n_x}, \ldots, \theta_{n_\phi n_x}\right] : \ \theta_{ij} \in \{\underline{\rho}_{ij}, \overline{\rho}_{ij}\}\},$$

where the bounds $\underline{\rho}_{ij}$ and $\overline{\rho}_{ij}$ are given in (14). From (21) and (22), the state estimation error dynamics can be rewritten as

$$e_{k+1} = \left(\mathscr{T}\mathscr{A}(h, \theta) - \mathscr{L}(h)C\right) e_k, \tag{23}$$

where

$$\begin{aligned} \mathscr{A}(h, \theta) &= \sum_{i=1}^{N} h_i(\xi_k)\mathscr{A}_i(\theta), \\ \mathscr{A}_i(\theta) &= A_i + \sum_{l=1}^{n_\phi} \sum_{j=1}^{n_x} \sigma_{n_\phi}(l)\sigma_{n_x}^{\top}(j)\theta_{lj}G_i. \end{aligned} \tag{24}$$

We are now ready to formulate the UIO design problem.

Problem 2. Consider the TS fuzzy system (12). Determine matrices of appropriate dimensions $\mathscr{T}$, $\mathscr{N}$ and $\mathscr{L}(h)$ of the TS fuzzy UI observer (16) such that both the state estimate $\hat{x}_k$ and the UI estimate $\hat{d}_k$ asymptotically converge to the state x_k and the UI d_k, respectively.

The following technical lemmas are useful for the design of TS fuzzy UI observers.

Lemma 2 ([42])**.** Given matrices of appropriate dimensions $\mathcal{A}$ and $\mathcal{B}$. There exists a matrix $\mathcal{X}$ such that $\mathcal{X}\mathcal{A} = \mathcal{B}$ if and only if $\mathcal{B}\mathcal{A}^{\dagger}\mathcal{A} = \mathcal{B}$. Moreover, the general solution to $\mathcal{X}\mathcal{A} = \mathcal{B}$ is given by

$$\mathcal{X} = \mathcal{B}\mathcal{A}^{\dagger} + \mathcal{Y}(I - \mathcal{A}\mathcal{A}^{\dagger}),$$

where $\mathcal{Y}$ is an arbitrary matrix of appropriate dimension.

Lemma 3 ([43])**.** Consider the MF-dependent inequality

$$\Upsilon_{hhh_+} = \sum_{i=1}^{N} \sum_{j=1}^{N} \sum_{l=1}^{N} h_i(\xi_k)h_j(\xi_k)h_l(\xi_{k+1})\Upsilon_{ijl} \succ 0, \tag{25}$$

where $h_+ = \left[h_1(\xi_{k+1}), h_2(\xi_{k+1}), \ldots, h_N(\xi_{k+1})\right]^{\top}$, and $h, h_+ \in \mathscr{H}$. The symmetric matrices of appropriate dimensions Υ_{ijl}, with $i, j, l \in \mathcal{I}_N$, are linearly dependent on the unknown decision variables. Inequality (25) holds if

$$\begin{aligned} & \Upsilon_{iil} \succ 0, \quad i, l \in \mathcal{I}_N \\ & \frac{2}{N-1}\Upsilon_{iil} + \Upsilon_{ijl} + \Upsilon_{jil} \succ 0, \quad i, j, l \in \mathcal{I}_N, \quad i \neq j. \end{aligned} \tag{26}$$

Note that Lemma 3 allows to convert the infinite LMI-based condition (25) in to a finite set of LMI constraints (26), which is numerically tractable.

B. LMI-Based Unknown Input Observer Design

The following theorem provides a numerical tractable solution for the UIO design in Problem 2.

Theorem 1. Consider the TS fuzzy system (12), there is an asymptotic UI observer in the form (16) if there exist matrices $\mathscr{T}$ and $\mathscr{N}$ satisfying conditions (17) and (20), and if there exist positive definite matrices $P_i \in \mathbb{R}^{n_x \times n_x}$, matrices $M_i \in \mathbb{R}^{n_x \times n_x}$, $L_i \in \mathbb{R}^{n_x \times n_y}$, for $i \in \mathcal{I}_N$, such that

$$\Phi_{iil}(\theta_p) \succ 0 \tag{27a}$$

$$\frac{2}{N-1}\Phi_{iil}(\theta_p) + \Phi_{ijl}(\theta_p) + \Phi_{jil}(\theta_p) \succ 0 \tag{27b}$$

for $i, j, l \in \mathcal{I}_N$, $i \neq j$, and $\theta_p \in \mathscr{V}_\phi$, $p \in \mathcal{I}_{2^{n_\phi} n_x}$. The quantity $\Phi_{ijl}(\theta_p)$ is given by

$$\Phi_{ijl}(\theta_p) = \begin{bmatrix} P_j & \star \\ M_j \mathscr{T} \mathscr{A}_i(\theta_p) - L_j C & M_j + M_j^\top - P_l \end{bmatrix},$$

with $\mathscr{A}_i(\theta_p)$ defined in (24). Moreover, the matrix $\mathscr{L}(h)$ in (16a) is defined as $\mathscr{L}(h) = M^{-1}(h)L(h)$ with

$$\begin{bmatrix} M(h) & L(h) \end{bmatrix} = \sum_{i=1}^{N} h_i(\xi_k) \begin{bmatrix} M_i & L_i \end{bmatrix}. \tag{28}$$

Proof. Note that if matrices $\mathscr{T}$ and $\mathscr{N}$ satisfy conditions (17) and (20), then the TS fuzzy UI observer (16) leads to the state estimation error dynamics (23). Moreover, conditions (17) and (20) can be rewritten in the compact form

$$\begin{bmatrix} \mathscr{T} & \mathscr{N} \end{bmatrix} \begin{bmatrix} I & D \\ C & 0 \end{bmatrix} = \begin{bmatrix} I & 0 \end{bmatrix}. \tag{29}$$

Due to the rank condition (15b), the solution of the algebraic matrix equation (29) exists. Applying Lemma 2 with

$$\mathcal{A} = \begin{bmatrix} I & D \\ C & 0 \end{bmatrix}, \quad \mathcal{B} = \begin{bmatrix} I & 0 \end{bmatrix}, \quad \mathcal{X} = \begin{bmatrix} \mathscr{T} & \mathscr{N} \end{bmatrix},$$

we can compute matrices $\mathscr{T}$ and $\mathscr{N}$ as

$$\begin{aligned} \begin{bmatrix} \mathscr{T} & \mathscr{N} \end{bmatrix} = \begin{bmatrix} I & 0 \end{bmatrix} \begin{bmatrix} I & D \\ C & 0 \end{bmatrix}^\dagger \\ + \mathcal{Y} \left(I - \begin{bmatrix} I & D \\ C & 0 \end{bmatrix} \begin{bmatrix} I & D \\ C & 0 \end{bmatrix}^\dagger \right), \end{aligned} \tag{30}$$

where $\mathcal{Y}$ is an arbitrary matrix of appropriate dimension.

For stability analysis, we consider the following MF-dependent Lyapunov function candidate:

$$\mathcal{V}(e_k) = e_k^\top P(h) e_k, \quad P(h) = \sum_{i=1}^{N} h_i(\xi_k) P_i. \tag{31}$$

By Lemma 3, it follows from (27a) and (27b) that

$$\begin{bmatrix} P(h) & \star \\ M(h)\mathscr{T}\mathscr{A}(h,\theta) - L(h)C & \mathscr{M}(h, h_+) \end{bmatrix} \succ 0, \tag{32}$$

for $h, h_+ \in \mathscr{H}$, $\theta \in \mathscr{S}_\phi$, with

$$\mathscr{M}(h, h_+) = M(h) + M(h)^\top - P(h_+),$$

and $P(h_+) = \sum_{i=1}^{N} h_i(\xi_{k+1}) P_i$. Since $P(h_+) \succ 0$, condition (32) implies $M(h) + M(h)^\top \succ 0$. This guarantees the existence of $M(h)^{-1}$, thus the validity of the expression of $\mathscr{L}(h)$.

Let us denote $\mathbf{A}(h,\theta) = \mathscr{T}\mathscr{A}(h,\theta) - \mathscr{L}(h)C = \mathscr{T}\mathscr{A}(h,\theta) - M(h)^{-1}L(h)C$. Premultiplying (32) with $\begin{bmatrix} I & -\mathbf{A}(h,\theta)^\top \end{bmatrix}$ on the left and its transpose on the right, we obtain

$$\mathbf{A}(h,\theta)^\top P(h_+) \mathbf{A}(h,\theta) - P(h) \prec 0. \tag{33}$$

Note that inequality (33) guarantees a negative variation of the fuzzy Lyapunov function (31) along the trajectory of the error dynamics (23), *i.e.*,

$$\begin{aligned} \delta\mathcal{V}_k &= \mathcal{V}(e_{k+1}) - \mathcal{V}(e_k) \\ &= e_{k+1}^\top P(h_+) e_{k+1} - e_k^\top P(h) e_k < 0, \ \forall k \in \mathbb{Z}_+. \end{aligned} \tag{34}$$

Using Lyapunov-based argument, it is clear that condition (34) guarantees the asymptotic stability of the error dynamics (23).

Hereafter, we show that the estimate $\hat{d}_k$ defined in (16c) converges asymptotically to the of the unknown input d_k. To this end, note from (12) that

$$d_k = (CD)^\dagger \left(y_{k+1} - C\Phi_k \right), \tag{35}$$

with $\Phi_k = A(h)x_k + f(\xi_k, u_k) + G(h)\phi(x_k, u_k)$. The UI estimation error $\varepsilon_k = d_k - \hat{d}_k$ can be computed from (16c) and (35) as

$$\varepsilon_k = (CD)^\dagger C \left(A(h)e_k + G(h)\delta_\phi \right). \tag{36}$$

Exploiting again expression (22), the UI estimation error ε_k in (36) can be rewritten in the form

$$\varepsilon_k = (CD)^\dagger C \mathscr{A}(h,\theta) e_k. \tag{37}$$

Since h and θ belong to *bounded* convex sets, *i.e.*, $h \in \mathscr{H}$ and $\theta \in \mathscr{S}_\phi$, remark from the *algebraic* equation (37) that if $e_k \to 0$, then $\varepsilon_k \to 0$. This concludes the proof. □

Remark 3. The observer design in Theorem 1 is recast as a convex optimization problem under strict LMI constraints (27). Hence, the decision matrices M_i, L_i, for $i \in \mathcal{I}_N$, constituting the observer gain $\mathscr{L}(h)$ as in (28), can be efficiently solved with available numerical toolboxes, for instance YALMIP package with SDPT3 solver [44].

The UI observer design is summarized in Algorithm 1. The proposed UI observer design can be now applied to the TS fuzzy model (10) for the estimation of vehicle nonlinear dynamics as described in Problem 1.

Algorithm 1: Observer Design Procedure

Input: Nonlinear system in the TS fuzzy form (12)
Output: Unknown input observer (16) such that $\hat{x}_k \to x_k$ and $\hat{d}_k \to d_k$, when $k \to \infty$

1. Check the matrix rank conditions in Assumption 2
   - If YES, then go to Step 2
   - If NO, then unapplicable algorithm
2. Compute matrices $\mathscr{T}$ and $\mathscr{N}$ from (30)
3. Solve LMI conditions (27) to get M_i, L_i, for $i \in \mathcal{I}_N$
4. Construct matrices $M(h)$ and $L(h)$ from (28)
5. Construct TS fuzzy unknown input observer (16)

IV. Hardware-in-the-Loop Experiments

This section presents real-time results obtained with HiL experiments to demonstrate the effectiveness of the proposed fuzzy UI observer design. Three test scenarios, representing different normal driving situations, are performed on a high-fidelity vehicle model to show the robustness of the new observer with respect to unmodeled vehicle dynamics.

A. Hardware-in-the-Loop Simulation Platform Setup

1) Full Vehicle Model: The real-time verification of the proposed nonlinear UI observer is performed with a 15-DOF multibody vehicle model [45], developed in LMS Imagine.Lab AMESim environment. This full vehicle model consists of a powertrain-chassis subsystem, a tire-road subsystem, a vehicle dynamics sensing subsystem and a vehicle control unit as depicted in Fig. 2. The key vehicle parameters are given in Table I while others are initialized by AMESim [45] to create a challenging simulation environment. The vehicle control unit is constructed in Simulink and embedded in AMESim via a co-simulation interface. Without further precision on the test scenarios, it is assumed that the vehicle drives on a flat ground with an ideal or a time-varying road adherence.

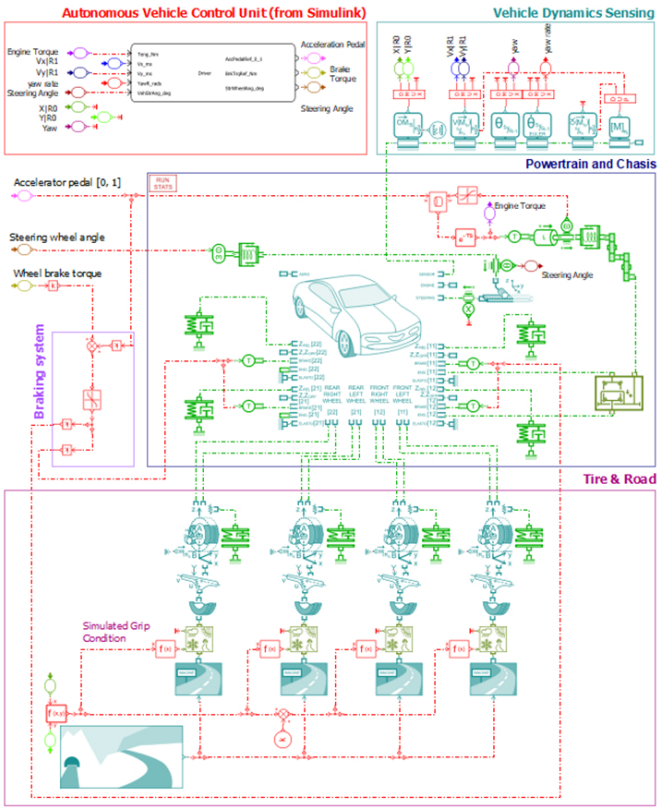

Fig. 2. AMESim full vehicle model running on HiL platform.

2) Hardware-in-the-Loop Platform Setup: To evaluate the practical estimation performance, a HiL platform has been setup as shown in Fig. 3(a). This platform consists of two real-time (RT) machines: a MicroAutoboxII (MABII) and a Vector System (VTS), and a personal computer to monitor and download programmes into the RT machines via their application tools: ControlDesk and CANoe/Pro. For the RT code generation, the MABII has been selected as the platform to run the full vehicle model while the VTS has been selected as the platform to function as the vehicle sensing system as well as to implement the designed fuzzy UI observer. All the programs have been implemented in Simulink, allowing RT code generation with RT interfaces from the dSPACE and the VTS, see Figs. 3(b) and (c), respectively. At each operation step, to mimic the practical automotive application, pulse-width modulation (PWM) output channels of the MABII are used to send the virtual sensor signals from the AMESim full vehicle model to the VTS. The VTS receives the MABII signals via its PWM input channels and converts them to physical signals.

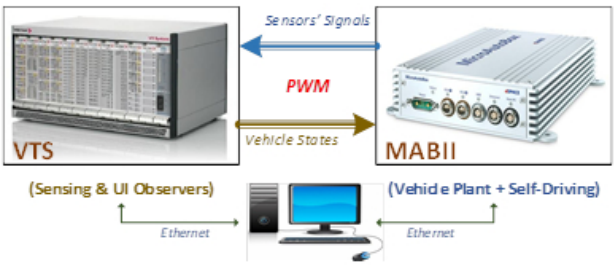

(a) Configuration of the HiL platform.

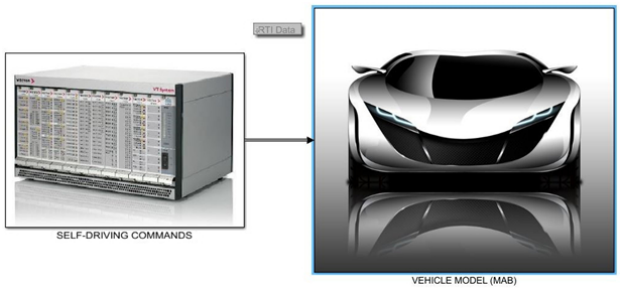

(b) Simulink design of the MABII.

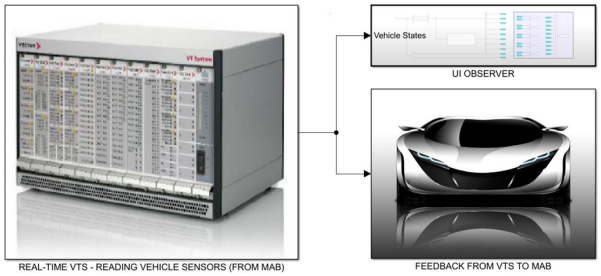

(c) Simulink design of the VTS.

Fig. 3. Hardware-in-the-loop platform setup.

B. Scenario 1: Driving with a Random Vehicle Trajectory

For this test scenario, the autonomous vehicle performs a driving task with a random trajectory and an increased acceleration after 14 [s] as shown in Figs. 4(a) and (b). Observe from Figs. 4(b), (c) and (d) that the estimated vehicle states quickly converge to their measured values. Moreover, Fig. 5 shows that both the unknown steering angle and the effective engine torque are accurately estimated with the proposed TS fuzzy observer.

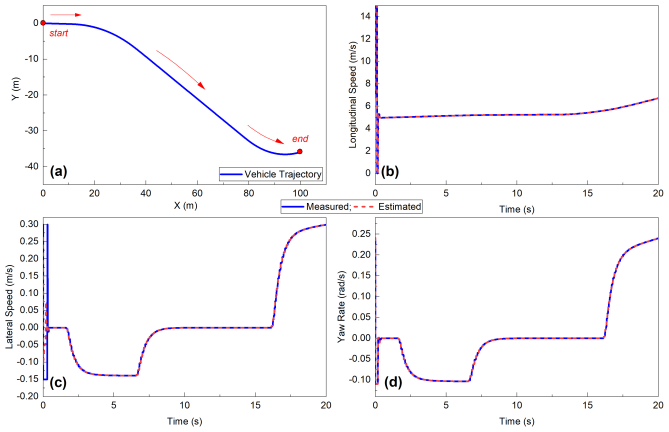

Fig. 4. Estimation performance in Scenario 1. (a) Vehicle trajectory. (b) Longitudinal speed v_x. (c) Lateral speed v_y. (d) Yaw rate r.

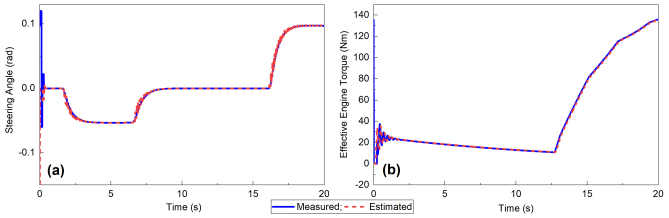

Fig. 5. Estimation performance in Scenario 1. (a) Steering angle δ. (b) Effective engine torque T_{eng}.

C. Scenario 2: Driving with a Circular Vehicle Trajectory

For this driving scenario, the estimation performance is tested with a circular trajectory as depicted in Fig. 6(a). The corresponding vehicle speed is given in Fig. 6(b). We can see that the unmeasured lateral speed and unknown vehicle inputs can be accurately reconstructed with the proposed fuzzy UI observer as shown in Fig. 6(c) and Fig. 7, respectively. Moreover, as in the previous driving scenario, the estimation convergence is very quick for all estimated vehicle variables.

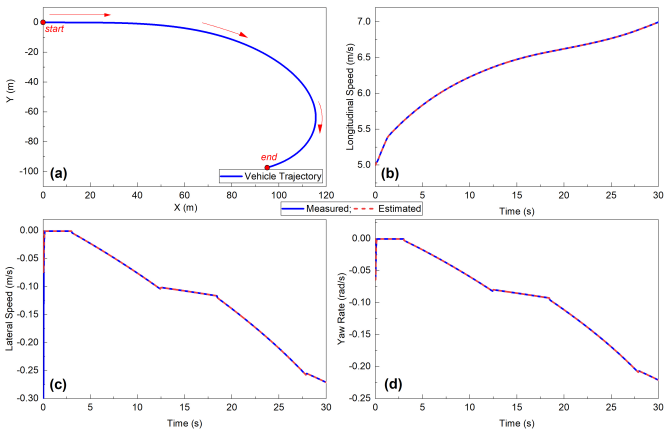

Fig. 6. Estimation performance in Scenario 2. (a) Vehicle trajectory. (b) Longitudinal speed v_x. (c) Lateral speed v_y. (d) Yaw rate r.

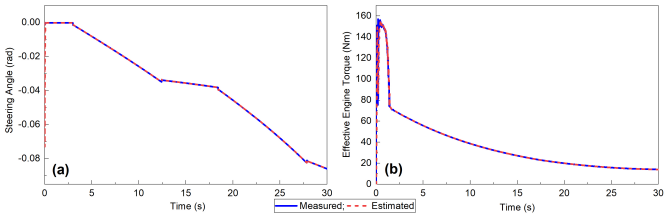

Fig. 7. Estimation performance in Scenario 2. (a) Steering angle δ. (b) Effective engine torque T_{eng}.

D. Scenario 3: Driving with a Time-Varying Road Adherence

This test is performed with a time-varying adherence condition to emphasize the robustness performance of the proposed UI observer. For this scenario, we assume that the autonomous vehicle performs a contour trajectory with radius varied from 45 [m] to 55 [m] and an increasing vehicle speed profile as shown in Figs. 8(a) and (b), respectively. To design a challenging driving situation, the interaction between the ground and the tires is now simulated by a road grip model as shown in Fig. 2, which is driven by the vehicle movement as

$$Road_{grip} = \mu_{grip}\left(1 + \sin\left(\frac{\pi\sqrt{X^2+Y^2}}{l_r}\right)\right),$$

where $\mu_{grip} = 0.6$ is the grip coefficient, X and Y are the vehicle positions. We can observe in Fig. 8 that the estimation of the vehicle states is also highly accurate in this situation. In particular, the proposed UI observer allows capturing precisely the high-frequency chattering behaviors of vehicle variables related to the lateral motion. The estimates of the steering angle and the effective engine torque also converges quickly to their respective measured signals as depicted in Fig. 9.

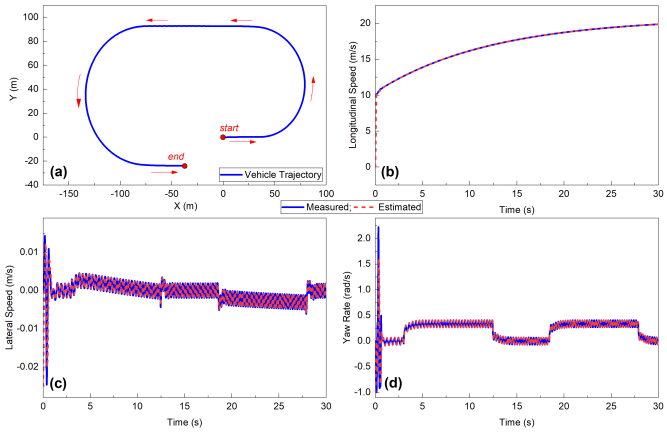

Fig. 8. Estimation performance in Scenario 3. (a) Vehicle trajectory. (b) Longitudinal speed v_x. (c) Lateral speed v_y. (d) Yaw rate r.

For a quantitative performance analysis, the mean absolute errors (respectively root mean square deviations) of the unmeasured lateral speed v_{yMAE}, steering angle δ_{MAE} and effective engine torque T_{engMAE} (respectively v_{yRMSD}, δ_{RMSD} and $T_{engRMSD}$) obtained with the proposed UI observer are computed. These performance indices are summarized in Table II for the three driving scenarios. The analysis results confirm that the proposed fuzzy UI observer can provide accurate

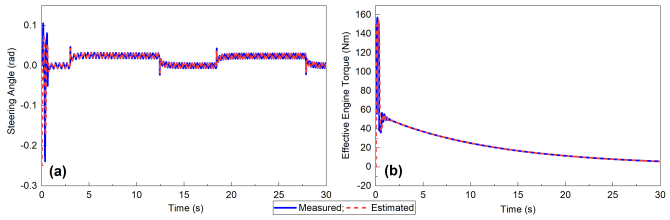

Fig. 9. Estimation performance in Scenario 3. (a) Steering angle δ. (b) Effective engine torque T_{eng}.

estimates of both vehicle state variables and unknown inputs under all considered test scenarios.

TABLE II
QUANTITATIVE ANALYSIS OF ESTIMATION PERFORMANCE.

Error index	Scenario 1	Scenario 2	Scenario 3
v_{yMAE} [m/s]	0.0025	5.66e-4	3.81e-4
δ_{MAE} [rad]	0.0018	9.71e-5	0.0023
T_{engMAE} [Nm]	0.9002	0.7329	0.7553
v_{yRMSD} [m/s]	3.81e-4	2.19e-4	2.96e-6
δ_{RMSD} [rad]	2.53e-4	2.91e-6	2.14e-4
$T_{engRMSD}$ [Nm]	5.164	5.212	5.319

V. CONCLUDING REMARKS

A new nonlinear UI observer design method has been proposed to simultaneously estimate the vehicle state, the lateral speed as well as the effective engine torque of autonomous ground vehicles. TS fuzzy modeling with nonlinear consequents is exploited for observer design to deal with the unmeasured nonlinearities of the combined longitudinal-lateral vehicle dynamics. The proposed generalized Luenberger observer structure permits an effective UI decoupling to guarantee an asymptotic convergence of both the vehicle state and the UI estimation errors. LMI-based observer design conditions are derived using Lyapunov arguments. The practical performance of the new fuzzy UI observer is real-time tested with a high-fidelity AMESim vehicle model. The results of HiL experiments show that the proposed nonlinear UI observer can provide accurate estimates of both vehicle state variables and UIs. Future works focus on the extension of the proposed estimation method to deal with limit driving situations, *e.g.*, by taking into account a nonlinear tire model or parametric uncertainties of the cornering stiffness parameters in the observer design. Moreover, exploiting the proposed UI observer structure for an effective fault-tolerant control scheme of autonomous vehicles is another promising research topic.

REFERENCES

[1] R. Rajamani, *Vehicle Dynamics and Control*. Springer US, 2012.

[2] Q. Shi and H. Zhang, "Fault diagnosis of an autonomous vehicle with an improved SVM algorithm subject to unbalanced datasets," *IEEE Trans. Indus. Electron.*, pp. 1–1, 2020, DOI: 10.1109/TIE.2020.2994868.

[3] A.-T. Nguyen, C. Sentouh, and J.-C. Popieul, "Driver-automation cooperative approach for shared steering control under multiple system constraints: Design and experiments," *IEEE Trans. Indus. Electron.*, vol. 64, no. 5, pp. 3819–3830, May 2017.

[4] H. Zhang, X. Huang, J. Wang, and H. R. Karimi, "Robust energy-to-peak sideslip angle estimation with applications to ground vehicles," *Mechatronics*, vol. 30, pp. 338–347, Sept. 2015.

[5] A.-T. Nguyen, C. Sentouh, and J.-C. Popieul, "Sensor reduction for driver-automation shared steering control via an adaptive authority allocation strategy," *IEEE/ASME Trans. Mechatron.*, vol. 23, no. 1, pp. 5–16, Feb. 2018.

[6] X. Wang, L. Guo, and Y. Jia, "Online sensing of human steering intervention torque for autonomous driving actuation systems," *IEEE Sens. J.*, vol. 18, no. 8, pp. 3444–3453, Apr. 2018.

[7] L. Li, F.-Y. Wang, and Q. Zhou, "Integrated longitudinal and lateral tire/road friction modeling and monitoring for vehicle motion control," *IEEE Trans. Intell. Transp. Syst.*, vol. 7, no. 1, pp. 1–19, Mar. 2006.

[8] E. Hashemi, M. Pirani, A. Khajepour, B. Fidan, A. Kasaiezadeh, and S. Chen, "Opinion dynamics-based vehicle velocity estimation and diagnosis," *IEEE Trans. Intell. Transp. Syst.*, vol. 19, no. 7, pp. 2142–2148, July 2018.

[9] D. Piyabongkarn, R. Rajamani, J. A. Grogg, and J. Y. Lew, "Development and experimental evaluation of a slip angle estimator for vehicle stability control," *IEEE Trans. Control Syst. Technol.*, vol. 17, no. 1, pp. 78–88, Jan. 2009.

[10] B. Zhang, H. Du, J. Lam, N. Zhang, and W. Li, "A novel observer design for simultaneous estimation of vehicle steering angle and sideslip angle," *IEEE Trans. Indus. Electron.*, vol. 63, no. 7, pp. 4357–4366, July 2016.

[11] W. Chen, D. Tan, and L. Zhao, "Vehicle sideslip angle and road friction estimation using online gradient descent algorithm," *IEEE Trans. Veh. Technol.*, vol. 67, no. 12, pp. 11 475–11 485, Dec. 2018.

[12] D. Selmanaj, M. Corno, G. Panzani, and S. M. Savaresi, "Vehicle sideslip estimation: A kinematic based approach," *Control Eng. Pract.*, vol. 67, pp. 1–12, Oct. 2017.

[13] M. Doumiati, A. C. Victorino, A. Charara, and D. Lechner, "Onboard real-time estimation of vehicle lateral tire-road forces and sideslip angle," *IEEE/ASME Trans. Mechatron.*, vol. 16, no. 4, pp. 601–614, Aug. 2011.

[14] K. Nam, S. Oh, H. Fujimoto, and Y. Hori, "Estimation of sideslip and roll angles of electric vehicles using lateral tire force sensors through RLS and Kalman filter approaches," *IEEE Trans. Indus. Electron.*, vol. 60, no. 3, pp. 988–1000, Mar. 2013.

[15] M. Gadola, D. Chindamo, M. Romano, and F. Padula, "Development and validation of a Kalman filter-based model for vehicle slip angle estimation," *Veh. Syst. Dyn.*, vol. 52, no. 1, pp. 68–84, 2014.

[16] M. Viehweger, C. Vaseur, S. van Aalst, M. Acosta, E. Regolin, A. Alatorre, W. Desmet, F. Naets, V. Ivanov, A. Ferrara *et al.*, "Vehicle state and tyre force estimation: demonstrations and guidelines," *Veh. Syst. Dyn.*, pp. 1–28, 2020.

[17] H. Du, J. Lam, K.-C. Cheung, W. Li, and N. Zhang, "Sideslip angle estimation and stability control for a vehicle with a non-linear tyre model and a varying speed," *Proc. Inst. Mech. Eng., Part D.*, vol. 229, no. 4, pp. 486–505, Feb. 2015.

[18] A.-T. Nguyen, T.-M. Guerra, C. Sentouh, and H. Zhang, "Unknown input observers for simultaneous estimation of vehicle dynamics and driver torque: Theoretical design and hardware experiments," *IEEE/ASME Trans. Mechatron.*, vol. 24, no. 6, pp. 2508–2518, Dec. 2019.

[19] B. Boada, M. Boada, and V. Diaz, "Vehicle sideslip angle measurement based on sensor data fusion using an integrated ANFIS and an unscented Kalman filter algorithm," *Mech. Syst. Signal Process.*, vol. 72, pp. 832–845, May 2016.

[20] X. Li, C. Chan, and Y. Wang, "A reliable fusion methodology for simultaneous estimation of vehicle sideslip and yaw angles," *IEEE Trans. Veh. Technol.*, vol. 65, no. 6, pp. 4440–4458, Jun. 2016.

[21] S. Cheng, L. Li, and J. Chen, "Fusion algorithm design based on adaptive SCKF and integral correction for side-slip angle observation," *IEEE Trans. Indus. Electron.*, vol. 65, no. 7, pp. 5754–5763, July 2018.

[22] A. Benloucif, A.-T. Nguyen, C. Sentouh, and J.-C. Popieul, "Cooperative trajectory planning for haptic shared control between driver and automation in highway driving," *IEEE Trans. Indus. Electron.*, vol. 66, no. 12, pp. 9846–9857, Dec. 2019.

[23] J. Si, Y. Niu, J. Lu, and H. Zhang, "High-precision estimation of steering angle of agricultural tractors using GPS and low-accuracy MEMS," *IEEE Trans. Veh. Technol.*, vol. 68, no. 12, pp. 11 738–11 745, Dec. 2019.

[24] J. Yang, E. Hou, and M. Zhou, "Front sensor and GPS-based lateral control of automated vehicles," *IEEE Trans. Intell. Transp. Syst.*, vol. 14, no. 1, pp. 146–154, Mar. 2013.

[25] S. Moon, I. Moon, and K. Yi, "Design, tuning, and evaluation of a full-range adaptive cruise control system with collision avoidance," *Control Eng. Pract.*, vol. 17, no. 4, pp. 442–455, Apr. 2009.

[26] J. Franco, M. Franchek, and K. Grigoriadis, "Real-time brake torque estimation for internal combustion engines," *Mech. Syst. Signal Process.*, vol. 22, no. 2, pp. 338–361, 2008.

[27] K. Hedrick, D. McMahon, V. Narendran, and D. Swaroop, "Longitudinal vehicle controller design for IVHS systems," in *American Control Conference*. Boston, MA, USA: IEEE, June 1991, pp. 3107–3112.
[28] Q. Ahmed and A. Bhatti, "Estimating SI engine efficiencies and parameters in second-order sliding modes," *IEEE Trans. Indus. Electron.*, vol. 58, no. 10, pp. 4837–4846, Oct. 2011.
[29] S. Helm, M. Kozek, and S. Jakubek, "Combustion torque estimation and misfire detection for calibration of combustion engines by parametric Kalman filtering," *IEEE Trans. Indus. Electron.*, vol. 59, no. 11, pp. 4326–4337, Nov. 2012.
[30] M. Hong, T. Shen, M. Ouyang, and J. Kako, "Torque observers design for SI engines with different intake air measurement sensors," *IEEE Trans. Control Syst. Technol.*, vol. 19, no. 1, pp. 229–237, Jan. 2011.
[31] J. Na, A. Chen, G. Herrmann, R. Burke, and C. Brace, "Vehicle engine torque estimation via UI observer and adaptive parameter estimation," *IEEE Trans. Veh. Technol.*, vol. 67, no. 1, pp. 409–422, Jan. 2018.
[32] K. Tanaka and H. Wang, *Fuzzy Control Systems Design and Analysis: a Linear Matrix Inequality Approach*. NY: Wiley-Interscience, 2004.
[33] A.-T. Nguyen, T. Taniguchi, L. Eciolaza, V. Campos, R. Palhares, and M. Sugeno, "Fuzzy control systems: Past, present and future," *IEEE Comput. Intell. Mag.*, vol. 14, no. 1, pp. 56–68, Feb. 2019.
[34] Q. Jia, W. Chen, Y. Zhang, and H. Li, "Fault reconstruction and fault-tolerant control via learning observers in Takagi-Sugeno fuzzy descriptor systems with time delays," *IEEE Trans. Indus. Electron.*, vol. 62, no. 6, pp. 3885–3895, 2015.
[35] J. Pan, A.-T. Nguyen, T.-M. Guerra, and D. Ichalal, "A unified framework for asymptotic observer design of fuzzy systems with unmeasurable premise variables," *IEEE Trans. Fuzzy Syst.*, pp. 1–1, 2020, DOI: 10.1109/TFUZZ.2020.3009737.
[36] A.-T. Nguyen, P. Coutinho, T.-M. Guerra, R. Palhares, and J. Pan, "Constrained output-feedback control for discrete-time fuzzy systems with local nonlinear models subject to state and input constraints," *IEEE Trans. Cybern.*, pp. 1–12, 2020, DOI: 10.1109/TCYB.2020.3009128.
[37] W. Jeon, A. Zemouche, and R. Rajamani, "Tracking of vehicle motion on highways and urban roads using a nonlinear observer," *IEEE/ASME Trans. Mechatron.*, vol. 24, no. 2, pp. 644–655, Apr. 2019.
[38] D. Swaroop and S. Yoon, "The design of a controller for a following vehicle in an emergency lane change maneuver," University of California, California PATH Working Paper UCB-ITS-PWP-99-3, Feb. 1999.
[39] Z. Wang, Y. Shen, X. Zhang, and Q. Wang, "Observer design for discrete-time descriptor systems: An LMI approach," *Syst. Control Lett.*, vol. 61, no. 6, pp. 683–687, 2012.
[40] A.-T. Nguyen, J. Pan, T.-M. Guerra, and Z. Wang, "Avoiding unmeasured premise variables in designing unknown input observers for Takagi-Sugeno fuzzy systems," *IEEE Control Syst. Lett.*, vol. 5, no. 1, pp. 79–84, 2021.
[41] G. Besançon, Ed., *Nonlinear Observers and Applications*, ser. Lecture Notes Control Inf. Sci. Springer-Verlag, 2007, vol. 363.
[42] A. Laub, *Matrix Analysis for Scientists and Engineers*. Philadelphia, PA, USA: SIAM, 2005, vol. 91.
[43] H.-D. Tuan, P. Apkarian, T. Narikiyo, and Y. Yamamoto, "Parameterized linear matrix inequality techniques in fuzzy control system design," *IEEE Trans. Fuzzy Syst.*, vol. 9, no. 2, pp. 324–332, 2001.
[44] J. Löfberg, "Yalmip: A toolbox for modeling and optimization in Matlab," in *IEEE Int. Symp. Comput. Aided Control Syst. Des.*, Taipei, Sept. 2004, pp. 284–289.
[45] J. Anthonis, M. Gubitosa, S. Donders, M. Gallo, P. Mas, and H. Van der Auweraer, *Recent Advances in Optimization and its Applications in Engineering*. Springer, Berlin, Heidelberg, 2010, ch. Multi-Disciplinary Optimization of an Active Suspension System in the Vehicle Concept Design Stage, pp. 441–450.

Anh-Tu Nguyen is an Associate Professor at the INSA Hauts-de-France, Université Polytechnique des Hauts-de-France, Valenciennes, France. He received the degree in engineering and the M.Sc. degree in automatic control from Grenoble Institute of Technology, France, in 2009, and the Ph.D. degree in automatic control from the Université Polytechnique Hauts-de-France, Valenciennes, France, in 2013.

After working a short period in 2010 at the French Institute of Petroleum, Rueil-Malmaison, France, Dr. Nguyen began his doctoral program at the University of Valenciennes, France, in collaboration with the VALEO Group. From February 2014 to August 2018, Dr. Nguyen was a postdoctoral researcher at the laboratory LAMIH UMR CNRS 8201, Valenciennes, France, and the laboratory LS2N UMR CNRS 6004, Nantes, France. Dr. Nguyen's research interests include robust control, constrained control systems, human-machine shared control for intelligent vehicles (see more information at https://sites.google.com/view/anh-tu-nguyen).

Truong Quang Dinh got the first-class B.E. mechatronics degree in the Mechanical Engineering Department at Hochiminh City University of Technology, Vietnam in March 2006. In 2010, he obtained Ph.D. degree from the School of Mechanical Engineering at University of Ulsan, South Korea. He worked as a postdoctoral researcher and as a Research Professor at the same university for several years. He is currently an Assistant Professor of WMG, University of Warwick, UK. His current research interests include energy system control.

Thierry-Marie Guerra is a Full Professor at the Polytechnic University Hauts-de-France, France. He received his PhD degree in automatic control in 1991 and the HDR in 1999. From 2009 to 2019, he was head of the Laboratory of Industrial and Human Automation, Mechanics and Computer Science (LAMIH CNRS UMR 8201) (148 researchers and staff, 110 PhD students and post-docs) http://www.univ-valenciennes.fr/LAMIH/. He is chair of the Technical Committee 3.2 "Computational Intelligence in Control" for IFAC, member of the IFAC TC 7.1 "Automotive Control", Area Editor of the international journals: Fuzzy Sets & Systems and IEEE Transactions on Fuzzy Systems. His research fields and topics of interest are wine, hard rock, stamps, nonlinear control, Takagi-Sugeno models control and observation, LMI constraints, nonquadratic Lyapunov functions and applications to mobility, soft robotics and disabled persons.

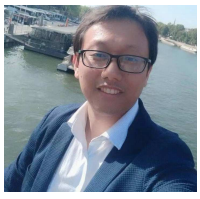

Juntao Pan received the B.Sc. degree in communication engineering and M.Sc. degree in control theory and control engineering from Three Gorges University, Yichang, China, in 2006 and 2008, respectively, and the Ph.D. degree in control theory and control engineering from Southeast University, Nanjing, China, in 2012.

He is currently an Associate Professor with North Minzu University, Yinchuan, China. His current research interests include fuzzy control, robust control, nonlinear control and their applications.